

Thin films of würtzite materials—AlN vs. AlP

Colin L. Freeman^a, Frederik Claeysens^a, Neil L. Allan^{a,*}, John H. Harding^b

^a*School of Chemistry, University of Bristol, Cantock's Close, Bristol BS8 1TS, UK*

^b*Department of Engineering Materials, University of Sheffield, Sir Robert Hadfield Building, Mappin Street, Sheffield S1 3JD, UK*

Available online 1 August 2006

Abstract

Ab initio periodic density functional calculations are reported of the polar (0001)/(000 $\bar{1}$) and non-polar (10 $\bar{1}$ 0) surfaces of AlN and AlP thin films. We analyse the optimised structures of the films in detail. These demonstrate the stabilisation of thicker films terminating with the polar (0001) surface via charge transfer and surface metallisation. The nature of the charge transfer is different in the two compounds and influences the observed relaxations of the surface atoms. For the (0001)/(000 $\bar{1}$) ultra-thin film of AlN, as for ZnO, the dipole is removed by the formation of a graphitic-like structure in which both Al and N are threefold coordinate. In contrast, the (0001)/(000 $\bar{1}$) ultra-thin film of AlP forms a “snake”-like structure with P present at both surfaces of the film. We discuss the possible implications of our results for the growth of the two materials.

© 2006 Elsevier B.V. All rights reserved.

PACS: 68.35.Bs; 73.20.At; 81.10.Aj; 81.15.Aa

Keywords: Al. Computer simulation; Al. Crystal morphology; Al. Nanostructures; B1. Nanomaterials; B1. Nitrides; B1. Phosphides

1. Introduction

Semiconductor materials with the würtzite structure are attracting substantial interest in a range of applications from light-emitting devices and solar cells to microsensors and photocatalysts. Key to many properties are the crystal size, orientation and the morphology. Growth of *c*-axis-orientated material is most common for AlN resulting in termination by the polar (0001)/(000 $\bar{1}$) surface under a range of growth conditions [1–4] and only very good epitaxy between film and substrate can limit growth to other non-polar surfaces [5]. AlP demonstrates polytypism with the zinc-blende structure (differing) from würtzite only in the *c*-axis stacking sequence (ABC vs. AB) and exhibits either the würtzite or the zinc-blende structure depending on small differences in the growth conditions [6,7]. In contrast to AlN and indeed other compounds with the würtzite structure (Fig. 1) including ZnO, ZnS, BeO, GaN and SiC, AlP often demonstrates epitaxy to the substrate when grown [8–10] and we have been unable to

find reports of the preference for the (0001)/(000 $\bar{1}$) morphology. Experimental studies of the surface structure of AlP find particularly rough surfaces which seem to form through a three-dimensional growth process involving multiple island growth rather than a two-dimensional layer by layer growth [9]. Controlling this growth to produce flat surfaces has proved difficult [8].

Several possible mechanisms for stabilising polar surfaces in würtzite systems have been suggested [11]. These include adsorption (e.g. of H atoms [12] in ZnO, or of N atoms in AlN) or vacancy formation. These possibilities have been examined by ab initio calculations for the (0001)/(000 $\bar{1}$) surfaces of AlN [13,14], which conclude that adsorption of a N atom between three surface Al atoms is most favoured for the Al-terminated (0001) surface while a N vacancy (forming a (2 × 2) surface unit cell) is preferred for the N-terminated (000 $\bar{1}$) surface. A further option is a change in the electronic structure of the surface layers as suggested for ZnO by Wander et al. [15] and Carlsson [16], and, most recently, more generally by Freeman et al. [17]. This involves charge transfer from the anion-terminated surface (usually the cation layer adjacent to the outmost anion layer) to the cation-terminated

*Corresponding author. Tel.: +44 117 9288308; fax: +44 117 925 0612.
E-mail address: n.l.allan@bris.ac.uk (N.L. Allan).

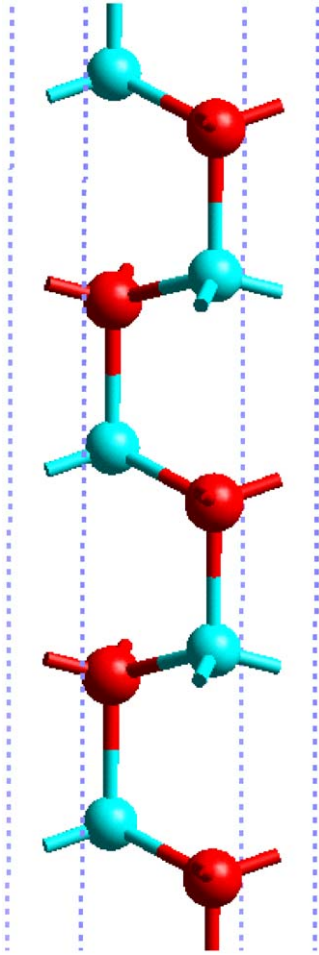


Fig. 1. Wurtzite structure of AlN. Here and in all subsequent figures, the cation is depicted in light blue and the anion is depicted in dark red.

surface. We have also previously noted [17] that ultra-thin (000 1)/(000 $\bar{1}$) films of AlN, BeO, GaN, SiC and ZnS are thermodynamically unstable with respect to a film with a graphitic-like structure and we have discussed the possible implications of this for the dominance of the growth by the (000 1)/(000 $\bar{1}$) films [18].

In this paper, we extend these studies and compare AlN and AIP in order to examine possible reasons for their different growth behaviour. Surface structure and stability are studied in detail and the structures adopted by very thin films investigated. We concentrate on undefective surfaces; non-stoichiometry and stabilisation by defects or adsorption are not considered. We note also that the only theoretical studies of AIP we have been able to find have focused on clusters [19,20] and so do not relate directly to the present study,

2. Methods

We chose to examine thin films of AlN and AIP terminating with the (000 1)/(000 $\bar{1}$) and (10 $\bar{1}$ 0) surfaces using the standard “supercell” method. Slabs periodic in two dimensions were separated with a vacuum gap of

approximately 12 Å; we tested for convergence with respect to the size of the gap. All the calculations were carried out using periodic plane-wave density functional theory with the generalised gradient approximation and the Perdew–Wang exchange correlation functional [21]. A cutoff of 380 eV was used for the plane-wave basis set. Ultra-soft Vanderbilt pseudopotentials [22] were used and the reciprocal space integration used the Monkhorst–Pack sampling scheme [23]. The calculations were performed with the CASTEP 4.2 code [24]. We have checked the convergence of the energy with the number of k -points.

The films were studied over a range of thicknesses. The number of layers present was increased from four until the surface energy of the film had converged for both the polar and non-polar surfaces.

3. Results and discussion

3.1. Non-polar (10 $\bar{1}$ 0) films

Both non-polar films are insulating. Calculated Mulliken charges for both systems, displayed in Table 1, show only a small difference between atoms at the surface and those in the interior. Significant relaxation for both AlN and AIP is limited to the three uppermost layers as listed in Table 2, which uses the labels shown in Fig. 2. In other layers, no bond length or angle changes by more than 1%. As is clear from Fig. 3, in the surface layer, the anions remain close to their bulk position while the outermost cations contract inward toward the slab, reducing the so-called dimer bond length in the surface layer (A in Fig. 2). This causes an increase in the tilt angle (θ) in the surface dimer bond (anion–Al–anion angle) away from the tetrahedral bond

Table 1
Calculated Mulliken charges for the (10 $\bar{1}$ 0) films

Film	Mean atomic charge within slab [e]		Atomic charge at slab surfaces [e]	
	Cation	Anion	Cation	Anion
AlN	+1.41	−1.41	+1.51	−1.47
AIP	+0.77	−0.77	+0.80	−0.70

“Within the slab” refers to all the atoms in the film excluding those in the surface layers.

Table 2
Variation of surface bond lengths and angles from their bulk values for (10 $\bar{1}$ 0) films of AlN (28 layers) and AIP (18 layers)

Film	Surface dimer bond length (A)	Average bilayer separation $((B + B')/2)$	Average layer separation $((C + C')/2)$	Tilt angle (θ)
AlN	−7.9%	−3.2%	+3.8%	+8.1°
AIP	−5.3%	−1.1%	+1.6%	+14.4°

Labels of distances and angles are as displayed in Fig. 2.

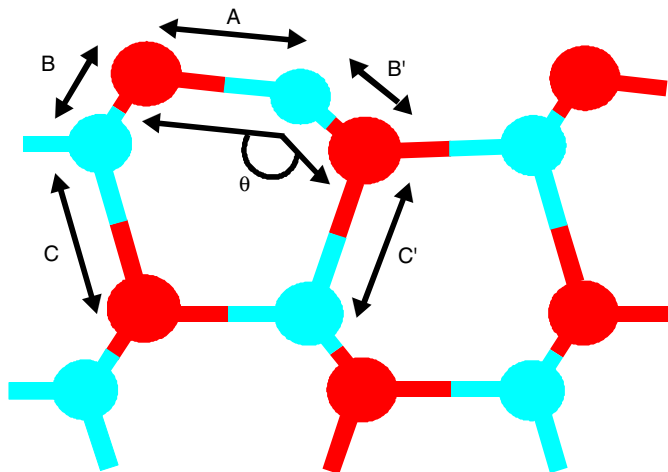


Fig. 2. Schematic representation of the relaxed $(10\bar{1}0)$ surface of AlN or AlP. Values of the distances and angle are recorded in Table 2.

angle. The tilt angle increases far more in AlP (123.8°) than in AlN (116.1°). The Al–X–Al angle decreases to 105.3° (X=N) and 94.7° (X=P), respectively, values associated with threefold N and P coordination more generally [25]. The anions and cations in the second layer move toward the surface, which decreases the separation between the atoms in the first layer and those in the second layer (B and B'). In the second layer, where the atoms remain fourfold coordinate, and unlike in the outermost layer where the coordinations are threefold, the Al–X–Al bond angles increase, markedly so for X=P (to $\approx 116^\circ$). The outward movement of the atoms in the second layer combined with a small inward movement of the atoms in the third layer increases the bond lengths between the atoms in the second layer and those in the third (C and C'). The bond lengths (A, B and B') reduce more in AlN than in AlP, which results in a greater increase in the separation between the second and third layers (C).

The DFT study of Filippetti et al. [26] reports broadly similar movements of the cations to our simulations for AlN, although they also report an upward shift away from the film of the surface layer anion which we do not observe. Nevertheless, their calculated tilt angle (θ) is 7.5° and the dimer contraction (A) is 7.5%, values which compare well with ours of 8.1° and 7.9% respectively. Previous theoretical studies have also suggested that the surface cations at the $(10\bar{1}0)$ surface of GaN move toward a threefold coordination consistent with increasing sp^2 -hybridisation [27,28], in line with our results. Unfortunately, we have found no studies of the non-polar surfaces of AlP.

3.2. Polar films

For AlN and AlP films terminating with the $(0001)/$ $(000\bar{1})$ polar surface and with more than 24 or 12 layers, respectively, geometry optimisation preserves the wurtzite structure. Both films are metallic and the charge distribu-

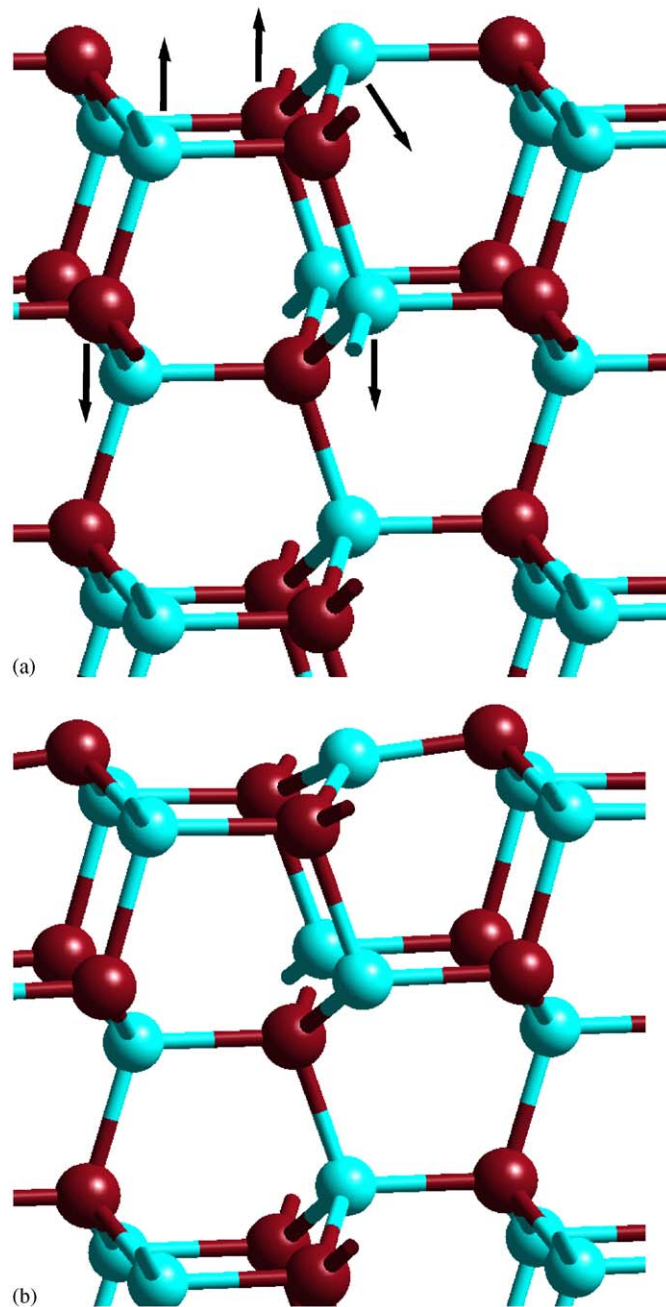


Fig. 3. Relaxations of the $(10\bar{1}0)$ surface of a 14-layer AlN slab. (a) The bulk structure before optimisation with arrows denoting the directions of the most significant atomic relaxations; (b) the optimised structure.

tion shows a charge transfer to remove the destabilising dipole as found also by Wander et al. [29] and Carlsson [16] at the analogous metallised surface of ZnO. There is a charge transfer from the valence band of the film to the empty conduction band, as shown schematically in Fig. 4.

The extent of the charge transfer does not vary with film thickness but changes from AlN to AlP. Results of Mulliken charge analyses on AlN and AlP films with 28 and 18 layers, respectively, are presented in Table 3. For AlN, there is little difference between the charges on N in the slab. The positive charge on Al varies far more, with a

range of $0.40e$, and there is a substantial decrease for Al in the layer adjacent to the $(000\bar{1})$ anion surface. Thus for AlN, the charge transfer is mainly from Al in the $(000\bar{1})$ surface bilayer to Al in the (0001) surface, where we define a surface bilayer as comprising the outermost layer and the adjacent, oppositely charged, layer. In contrast, in the AlP films, the variations of the charges on P and Al are comparable, $0.43e$ and $0.47e$ respectively. The charges on the P at the $(000\bar{1})$ surface and the Al at the (0001) surface do not change very much from those in the slab interior. The charge transfer is mainly from the Al in the $(000\bar{1})$ surface bilayer to the P in the (0001) surface bilayer, uniquely of the seven wurtzite $(0001)/(000\bar{1})$ surfaces of AlN, AlP, ZnO, ZnS, SiC, GaN and BeO we have studied either in this paper or previous work [17,18].

Table 4 lists the surface relaxations at both the cation- and anion-terminated surfaces, using labels explained in Fig. 5. At the $(000\bar{1})$ (anion) surface of both AlN and AlP, the bonds between layers within each bilayer contract (G), while the bonds between the bilayers (H) expand; the bond angle (ϕ) within each bilayer also increases. For AlN at the (0001) (cation) surface, G and ϕ are virtually unchanged while H increases (by less than for $(000\bar{1})$); for AlP, the changes at the (0001) surface are qualitatively the same as at $(000\bar{1})$. The relaxations of the atoms not in the surface bilayers from their bulk positions are generally small ($<1\%$). We have been unable to find any experimental or

theoretical studies for “clean” polar surfaces with which to compare our calculated geometries.

There is more variation in behaviour here than for the non-polar surface and in part this is due to the marked charge transfers that stabilise the polar surface. At the anion-terminated surface, the increased charge on the Al in the adjacent layer pulls in the outermost 3-coordinate nitrogen; G decreases and ϕ (at this surface the Al–anion–Al angle) increases consistent with increasing sp^2 -hybridisation. Distance H increases considerably here too, weakening the interaction between the surface bilayer and subsequent layers. This is more pronounced for the N than the P-terminated surface consistent with the reluc-

Table 4
Relaxations of the surface atoms for AlN (28 layers) and AlP (18 layers) $(0001)/(000\bar{1})$

Film	G_{cation}	G_{anion}	H_{cation}	H_{anion}	ϕ_{cation}	ϕ_{anion}
AlN	+0.1%	−3.3%	+1.1%	+5.4%	−0.3°	+5.7°
AlP	−1.6%	−1.8%	+2.2%	+3.3%	+3.3°	+3.6°

Subscript refers to the particular surface, e.g. G_{cation} is the change in G at the cation-terminated (0001) surface.

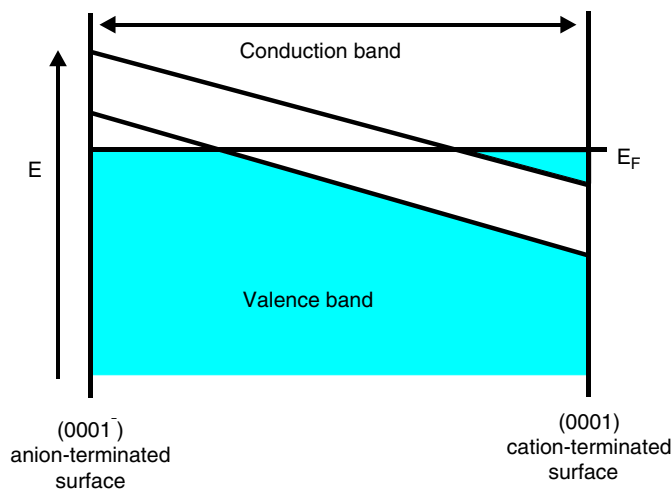


Fig. 4. Schematic representation of the charge transfer process that occurs in the polar $(0001)/(000\bar{1})$ films of AlN and AlP.

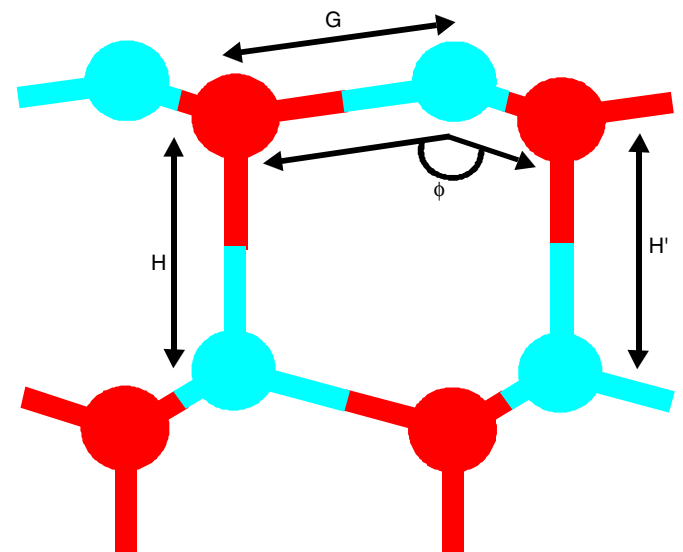


Fig. 5. Schematic representation of the relaxed $(000\bar{1})$ surface of AlN or AlP. The distances and angle are recorded in Table 2.

Table 3

Mean Mulliken charges on atoms within the AlN (28 layers) and AlP (18 layers) $(0001)/(000\bar{1})$ films (excluding the two surface bilayers, i.e. the surface layer and the layer adjacent to it)

Film	Mean atomic charge within slab [e]		(0001) Surface bilayer [e]		$(000\bar{1})$ Surface bilayer [e]	
	Cation	Anion	Cation	Anion	Cation	Anion
AlN	+1.43	−1.43	+1.19	−1.43	+1.59	−1.34
AlP	+0.79	−0.79	+0.78	−1.18	+1.25	−0.75

Also listed are the charges of the anions and cations in the surface bilayers.

tance of 3-coordinate P for multiple interlayer bonding and its preference for retaining a pyramidal coordination. At the Al-terminated surface in AlN, the decrease in positive charge on the outermost Al contributes to the overall small changes in G and ϕ . In AlP, in contrast, the P atoms in the surface bilayer are considerably more negatively charged and pull in the outermost Al; G decreases and ϕ (at this surface the Al–anion–Al angle) increases.

3.3. Ultra-thin polar films

The (0001)/(000 $\bar{1}$) films of AlN with less than 24 layers behaved very different from the thicker films. These underwent a massive relaxation to the non-polar and insulating graphitic-like structure we have previously seen in analogous calculations for ZnO films (with less than 18 layers) [18]. This graphitic structure arises from the atoms within a bilayer converging to one layer, e.g. an eight-layer (0001)/(000 $\bar{1}$) film will become a four-layer graphitic film (although we shall continue to refer to it as an eight-layer film for comparison with the other films) with a ABAB... stacking sequence (Fig. 6). We have only been able to find one previous reference to flat films for würtzite-based

materials other than our own for ZnO. This is a DFT calculation [30] for four-layer GaN on SiC.

The relaxations required to form the new graphitic morphology are large. The interatomic distances within the new layers are smaller (1.844 Å) but the separation between the layers is substantially larger (2.093 Å) than in the (0001)/(000 $\bar{1}$) film. The bond angles within a layer are hexagonal, $\approx 120^\circ$, and are $\approx 90^\circ$ between layers. We observe no variation of the geometry with film thickness.

We have previously noted that the surface relaxations of the (0001)/(000 $\bar{1}$) and (10 $\bar{1}$ 0) films of AlN both change the surface geometry toward a sp^2 -like geometry, increasing the separation between the surface bilayer and the next layer (distances H and C for the polar and non-polar surfaces, respectively). In this context, the formation of the graphitic structure can be seen simply as an extreme example of this type of relaxation, now affecting the entire film.

The ultra-thin films of (0001)/(000 $\bar{1}$) AlP behave very differently. For films of less than 14 layers, the “snake”-like structure shown in Fig. 7 is obtained. Rather than adopt a flat geometry the 3-coordinate P atoms adopt a non-planar pyramidal geometry in keeping with the molecular chemistry [25] of P with P–Al–P angles of $\approx 74^\circ$ between the layers and $\approx 112^\circ$ within the layers. The structure still contains six-membered rings (in a chair conformation). The destabilising dipole is removed since alternate bilayers in the polar films have inverted; P is the outermost atom at both surfaces of the film. The snake structure is higher in energy than the würtzite structure for

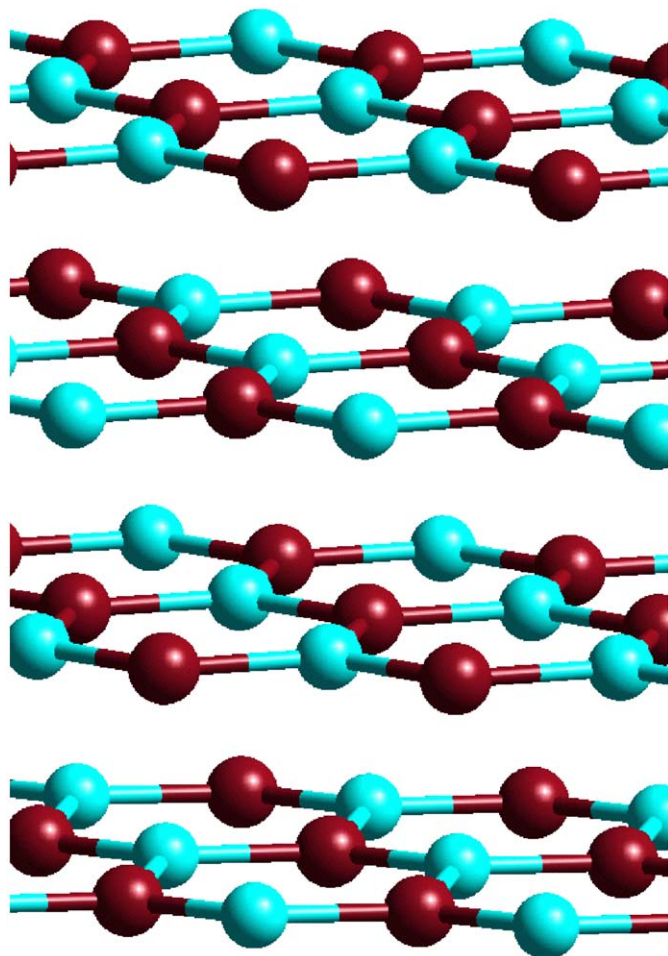


Fig. 6. Graphitic AlN structure.

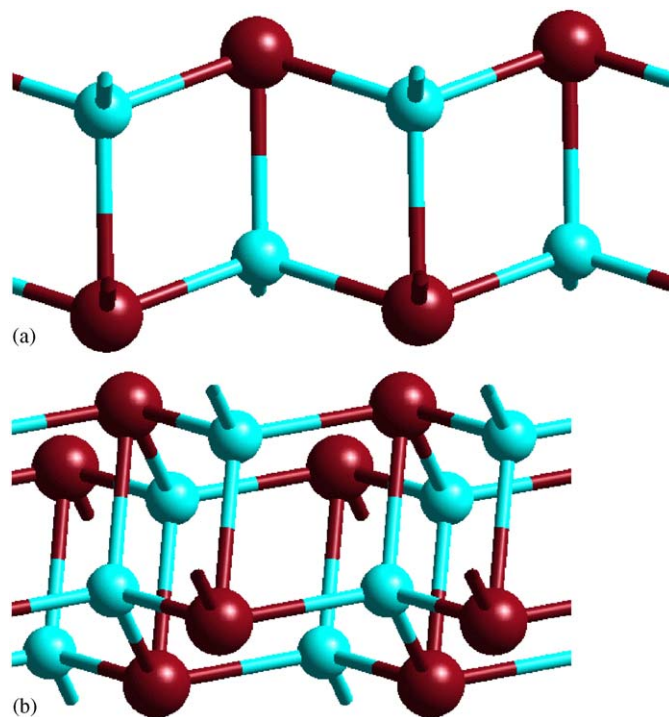


Fig. 7. Side views of the snake structure observed for a 4-layer film of AlP. (a) Side view of structure from the [100] direction. (b) Film tilted to show bonding arrangement in the [100] direction.

all film thicknesses of 14 layers or more and optimisation of these films produces the polar (0001)/(000 $\bar{1}$) films discussed above. Like the graphitic structure, the snake structure is insulating.

3.4. Cleavage energies

Cleavage energies were calculated for each of the films using the energy of the films and the energy of the bulk wurtzite crystal (including the graphitic film). Note that since both (0001) and (000 $\bar{1}$) surfaces are present in the film, no unique surface energy can be determined for either surface by itself. For the non-polar surface, the cleavage energy is just twice the surface energy. Fig. 8 shows plots of the variation of the cleavage energy with the number of layers present in the film for all the films studied.

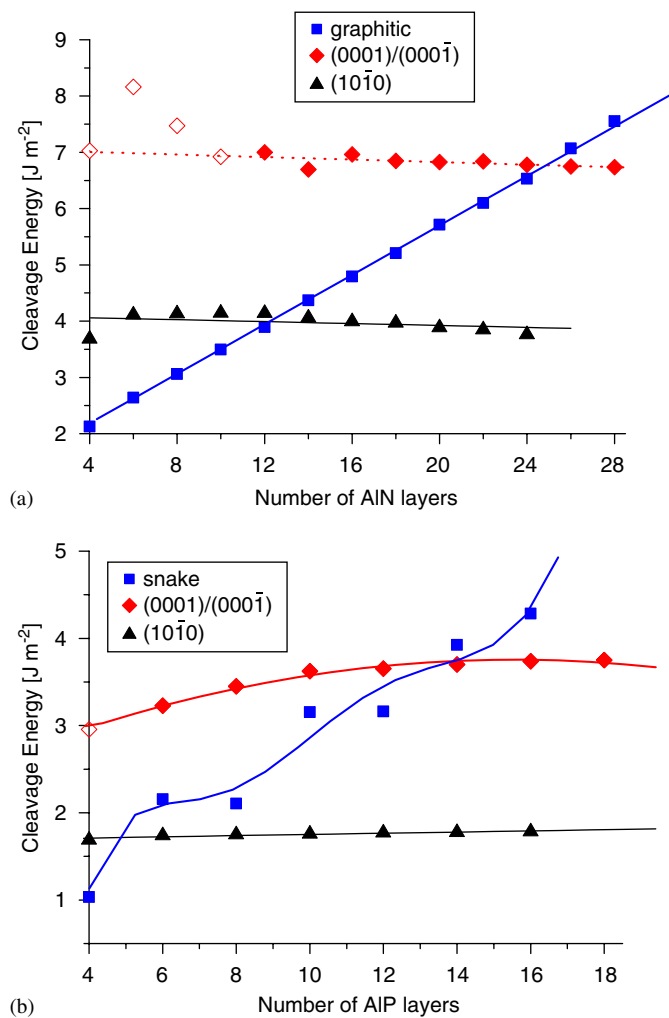


Fig. 8. Cleavage energies as a function of film thickness for (a) AlN and (b) AlP. For the graphitic surface, the number of layers plotted is that *before* optimisation. For a small number of layers, the (0001)/(000 $\bar{1}$) films are unstable with respect to the graphitic and snake structures. These particular values are plotted as open diamonds and were obtained by relaxation with a set of constraints that prevent the film optimising to the graphitic or snake structure.

The non-polar (10 $\bar{1}$ 0) film has a lower cleavage energy than the polar (0001)/(000 $\bar{1}$) film for all thicknesses. The differences are $\approx 3 \text{ J m}^{-2}$ and $\approx 2 \text{ J m}^{-2}$ for AlN and AlP, respectively. Interestingly, the graphitic structure observed for AlN is lower in energy than the (10 $\bar{1}$ 0) surface for films of less than 14 layers, while the snake structure of AlP is only lower in energy than the (10 $\bar{1}$ 0) surface for films with four layers or less.

Given the form of the graph in Fig. 8 for AlN, it appears surprising that the observed morphology is dominated by the polar surface. However, the analogous plot for ZnO, for which this surface also dominates the morphology, is similar [18]. We have discussed this issue in detail for ZnO previously and the same growth model could apply here. The initial deposition of AlN should produce the graphitic structure. When the number of layers present within the film exceeds 12 then, on thermodynamic grounds only, we would expect a conversion to the lower energy (10 $\bar{1}$ 0) film. However, the large structural differences between the graphitic and (10 $\bar{1}$ 0) structure suggests any interconversion between these will involve a substantial energy barrier, as suggested by suitable estimates of the energetics of the transformation pathway [18] for ZnO. For AlN, eventually, beyond 24 layers the surface energy of the graphitic structure exceeds that of the (0001)/(000 $\bar{1}$) film. Conversion from the graphitic to the (0001)/(000 $\bar{1}$) film only requires the buckling of the graphitic sheets and would be expected to have a small energy barrier; we have found no energy barrier for the transition between the graphitic and (0001)/(000 $\bar{1}$) films (for more than 24 layers).

Thus, as the layer depth increases, the graphitic film converts to the thermodynamically more stable polar (0001)/(000 $\bar{1}$)-terminated structure. Effectively, the graphitic layers prevent the formation of the lower energy films terminated with non-polar surfaces.

We find no reports for AlP demonstrating the same preference for the (0001)/(000 $\bar{1}$) morphology as the other wurtzite materials we have studied, and the calculations indicate that the graphitic structure is unstable for AlP. Optimisation of a graphitic structure results in a transition to either the snake structure (thin films) or the polar-terminated solution (thicker films). The growth model described above for ZnO and AlN cannot apply to AlP. Since the snake structure is lowest in energy for the four-layer film, we may expect that the initial deposition of AlP produces this structure. As the film thickness increases, thermodynamic considerations would suggest conversion to the (10 $\bar{1}$ 0) surface. The snake structure is not as structurally different from the (10 $\bar{1}$ 0) surface as the graphitic. As the AlP film increases in thickness, the snake structure becomes energetically unfavourable in comparison with the other potential surfaces. But in contrast to AlN, there is no clear kinetic argument to direct the growth into one particular surface direction since all conversions require either translations of layers relative to each other or inversions of layers and are likely to possess an energy barrier. Thus, we do not see the same preference for one

particular surface. Experimental studies do not observe the same exclusive preference to one surface that is found in AlN and AlP often demonstrates epitaxy with the surface medium [8–10]. These results are fully consistent with our calculations.

4. Conclusions

We have used ab initio calculations to model the polar (0001)/(000 $\bar{1}$) and non-polar (10 $\bar{1}$ 0) surfaces of AlN and AlP thin films. We demonstrate that the charge transfer model proposed by Wander et al. [29] and Carlsson [16] for the stabilisation of the polar (0001) and (000 $\bar{1}$) surfaces of ZnO can also operate for AlN and AlP. The charge analysis of AlN suggests that the charge transfer occurs from the Al in the (000 $\bar{1}$) layer to the Al in the (0001) layer so the N are largely unaffected by the stabilisation process. In AlP in contrast, it appears that charge transfer occurs from the Al in the (000 $\bar{1}$) surface bilayer to the P in the (0001) surface bilayer. For both the polar and non-polar surfaces, we have recorded surface relaxations which change the surface atom geometry from sp³ to a sp²-like geometry.

For the (0001)/(000 $\bar{1}$) ultra-thin film of AlN, the dipole is removed by the formation of a new graphitic structure, again as for ZnO [18]. In contrast, the (0001)/(000 $\bar{1}$) ultra-thin film of AlP forms a “snake”-like structure with P present at both surfaces of the film. We have considered the possible implications of these two structures for the growth of AlN and AlP.

Acknowledgements

The authors would like to thank EPSRC for funding (Grant nos. GR/85952 and GR/85969).

References

- [1] Z. Sitar, L.L. Smith, R.F. Davis, *J. Crystal Growth* 141 (1994) 11.
- [2] A. Sasaki, J. Liu, W. Hara, S. Akiba, K. Saito, T. Yodo, M. Yoshimoto, *J. Mater. Res.* 19 (2004) 2725.
- [3] B.J. Kowalski, R.J. Iwanoski, J. Sadowski, I.A. Kowalik, J. Kanski, I. Grzegory, S. Porowski, *Surf. Sci.* 548 (2004) 220.
- [4] M.E. Lin, S. Strite, A. Agarwal, A. Salvador, G.L. Zhou, N. Teraguchi, A. Rockett, H. Morkoç, *Appl. Phys. Lett.* 62 (1993) 702.
- [5] W.A. Melton, J.I. Pankove, *J. Crystal Growth* 178 (1997) 168.
- [6] Y.-Z. Yoo, T. Chikyow, P. Ahmet, Z.-W. Jin, M. Kawasaki, H. Koinuma, *J. Crystal Growth* 237–239 (2002) 1594.
- [7] T.B. Nasrallah, M. Amlouk, J.C. Bernede, S. Belgacem, *Phys. Status Solidi A* 201 (2004) 3070.
- [8] M. Ishii, S. Iwai, T. Ueki, Y. Aoyagi, *Thin Solid Films* 318 (1998) 6.
- [9] M. Ishii, S. Iwai, T. Ueki, Y. Aoyagi, *Appl. Phys. Lett.* 71 (1997) 1044.
- [10] D. Rickman, *J. Electrochem. Soc.* 115 (1968) 945.
- [11] C. Noguera, *J. Phys.: Condens. Matter* 12 (2000) R367.
- [12] M. Kunat, S.G. Girol, T. Becker, U. Burghaus, C. Wöll, *Phys. Rev. B* 66 (2002) 081402.
- [13] J. Fritsch, O.F. Sankey, K.E. Schmidt, J.B. Page, *Phys. Rev. B* 57 (1998) 15360.
- [14] J.E. Northrup, R. Di Felice, J. Neugebauer, *Phys. Rev. B* 55 (1997) 13878.
- [15] A. Wander, P. Schedin, P. Steadman, A. Norris, R. Mcgrath, T.S. Turner, G. Thornton, N.M. Harrison, *Phys. Rev. Lett.* 86 (2001) 3811.
- [16] J.M. Carlsson, *Comput. Mater. Sci.* 22 (2001) 24.
- [17] C.L. Freeman, F. Claeysens, N.L. Allan, J.H. Harding, *Phys. Rev. Lett.* 96 (2006) 066102.
- [18] F. Claeysens, C.L. Freeman, N.L. Allan, Y. Sun, M.N.R. Ashfold, J.H. Harding, *J. Mater. Chem.* 15 (2005) 139.
- [19] A. Tomasulo, M.V. Ramakrishna, *J. Chem. Phys.* 105 (1996) 10449.
- [20] L. Guo, H.-S. Wu, Z.-H. Jin, *J. Mol. Struct.* 684 (2004) 67.
- [21] J.P. Perdew, Y. Wang, *Phys. Rev. B* 45 (1992) 13244.
- [22] D. Vanderbilt, *Phys. Rev. B* 41 (1990) 7892.
- [23] H.J. Monkhorst, J.D. Pack, *Phys. Rev. B* 13 (1976) 5188.
- [24] M.C. Payne, M.P. Teter, D.C. Allan, T.A. Arias, J.D. Joannopoulos, CASTEP 4.2, academic version, licensed under the UKCP-MSI Agreement, 1999, *Rev. Mod. Phys.* 64 (1992) 1045.
- [25] N.N. Greenwood, A. Earnshaw, *Chemistry of the Elements*, second ed., Reed Educational and Professional Publishing Ltd., Oxford, 1997.
- [26] A. Filippetti, V. Fiorentini, G. Cappellini, A. Bosin, *Phys. Rev. B* 59 (1999) 8026.
- [27] J.E. Jaffe, R. Pandey, P. Zapol, *Phys. Rev. B* 53 (1996) R4209.
- [28] J.E. Northrup, J. Neugebauer, *Phys. Rev. B* 53 (1996) R10477.
- [29] A. Wander, F. Schedin, P. Steadman, A. Norris, R. Mcgrath, T.S. Turner, G. Thornton, N.M. Harrison, *Phys. Rev. Lett.* 86 (2001) 3811.
- [30] R.B. Capaz, H. Lim, J.D. Joannopoulos, *Phys. Rev. B* 51 (1995) 17775.